



E-ISSN: 2321-2187

P-ISSN: 2394-0514

[www.florajournal.com](http://www.florajournal.com)

IJHM 2020; 8(5): 125-133

Received: 22-07-2020

Accepted: 24-08-2020

**Monique Gonçalves Alves**

Faculty of Medicine, University of São Paulo, FMUSP, Laboratory of Development and Innovation, Butantan Institute Sao Paulo, Brazil

**Laertty Garcia de Sousa Cabral**

Faculty of Medicine, University of São Paulo, FMUSP, Laboratory of Development and Innovation, Butantan Institute Sao Paulo, Brazil

**Luiza Stolz Cruz**

Department of Pharmaceutical Sciences, University of Ponta Grossa, Ponta Grossa, Brazil

**Flávio Luís Beltrame**

Department of Pharmaceutical Sciences, University of Ponta Grossa, Ponta Grossa, Brazil

**Arthur Cássio de Lima Luna**

University Nove de Julho, UNINOVE, São Paulo, Brazil

**Durvanei Augusto Maria**

Laboratory of Development and Innovation, Butantan Institute Sao Paulo, Brazil

**Corresponding Author:**

**Durvanei Augusto Maria**  
Laboratory of Development and Innovation, Butantan Institute Sao Paulo, Brazil

## Induced antiproliferative responsive by fraction of *Euphorbia umbellata* latex inhibits melanoma tumor cells

**Monique Gonçalves Alves, Laertty Garcia de Sousa Cabral, Luiza Stolz Cruz, Flávio Luís Beltrame, Arthur Cássio de Lima Luna and Durvanei Augusto Maria**

**Abstract**

The objective was to evaluate the antitumor potential of the Chloroform (CHCl<sub>3</sub>) and Acetate (CH<sub>3</sub>COO) fractions of *Euphorbia umbellata* latex in melanoma tumor cells (B16-F10) and comparative effect normal fibroblast cells (FN1). The cytotoxicity of the fractions in B16-F10 and normal FN1 cells was evaluated using the MTT colorimetric method, mitochondrial electrical potential ( $\Delta\Psi_m$ ), analysis of organization of cytoskeleton by confocal microscopy and cell cycle phases by flow cytometry. The Acetate fraction obtained greater selectivity for B16-F10 tumor cells, reduced  $\Delta\Psi_m$  and modified cell morphology, observed by actin filaments. Our results suggest that Acetate and Chloroform can inhibit the proliferation of tumor cells of melanoma B16-F10, promoting apoptosis and inducing a control of proliferation. The Acetate fraction modulating apoptotic pathways and disrupting of organization cytoskeleton.

**Keywords:** *Euphorbia umbellata*, melanoma, apoptosis, DNA fragmented

**1. Introduction**

Melanoma is the most aggressive skin cancer. The tumor microenvironment modulates several mechanisms that promote intrinsic growth, with an overall mortality rate of approximately 20%, is responsible for 80% of skin cancer-related deaths worldwide, with a median overall survival of six months [1, 2]. In Brazil, according to the Cancer National Institute (INCA), despite corresponding to 3% of the 30% of all malignant skin tumors registered in the country, melanoma is considered the most aggressive type of skin cancer due to its high metastatic potential [3].

Although considered chemoresistant, traditional chemotherapy has long been the only option available [4]. Dacarbazine, despite being well tolerated, has a response of only 20%, whereas combined chemotherapy produces better responses, but does not prolong survival and is normally associated with greater toxicity, whereas immunotherapy with high doses of IL-2 produces responses more lasting therapies in only a small percentage of patients [5].

In the past few years, two distinct classes of therapies have completely changed strategies in the treatment of melanoma. One of these classes corresponds to the target therapies, represented by the BRAF-V600 mutation inhibitor, or the proteins involved in the MAPKs signaling pathway (MEK-ERK), which are treatment options for about 40-50% of the types of melanoma [6]. However, despite advances in recent decades, patients treated with BRAF inhibitors show disease progression during the first 1 to 2 years of therapy [6]. Also, the duration of the response is relatively short or the response to treatment is low [7].

Resistance to currently available therapies searches for new adjuvant drugs even more attractive [8]. In this perspective, natural bioactive, derived from leaves, roots, barks, or stems of plants, which are used in traditional medicine to treat various diseases, may become therapeutic alternatives or adjuvant the treatment of numerous types of cancer [9].

Recent studies describe the properties of plant extracts from species of the Euphorbiaceae family that are popularly used to treat different types of cancer, ulcers, and other diseases. The cytotoxic activity of *Cnidioscolus quercifolius* against tumor cells of the prostate (PC3 AND PC3-M) and breast (MCF-7) showed relevant cytotoxic activity, with a high content of flavonoids is one of the extracted fractions [10]. In the same way that *Euphorbia bicolor* extract and, phytochemicals significantly reduced the growth of breast cancer cells MCF-7 and T47D luminal A ER<sup>+</sup> PR<sup>+</sup> HER2<sup>-</sup>, *Claudin-low* MDA-MB231 ER<sup>-</sup> PR<sup>-</sup> HER2<sup>-</sup> claudin-3 claudinin-4,7 low and MDA-MB 468 basal ER<sup>-</sup> PR<sup>-</sup> HER2<sup>-</sup> [11].

Within this family, the plant *Euphorbia umbellata* (Pax) Bruyns, Euphorbiaceae [12] popularly known in Brazil as "cola-nota" or "janaúba" has demonstrated cytotoxic effects from its latex. Fractions such as hexane (Hex), chloroform (CHCl<sub>3</sub>), ethyl acetate and methanol (MeOH) extracted from their latex, were isolated for pharmacological evaluation and demonstrated antitumor potential in several types of cancer, such as tumor cells of ileocecal colorectal adenocarcinoma (HCT- 8), human cervical tumor (HeLa), Jurkat cells (Leukemia), hepatocarcinoma cells (Hepa) and triple-negative human breast cancer (MDA MB-231) [12-15].

In B16-F10 melanoma cells, studies with the hexane and fraction and ether, methanol, and dichloromethane subfractions extracted from *Euphorbia umbellata* latex have the high cytotoxic potential for these cells [16-15]. In this context, with the possibility that other active compounds present in its latex may have antitumor properties; the objective of the work was to evaluate the antitumor potential of the chloroform (CHCl<sub>3</sub>) and acetate (CH<sub>3</sub>COO-) fractions.

## 2. Methodology

### 2.1. Cell culture

The cells of the melanoma B16-F10 (ATCC<sup>®</sup> CRL-6475<sup>™</sup>) and normal human fibroblast (FN1) strains were cultured in RPMI-1640, pH 7.2 culture medium, supplemented with 10% inactivated fetal bovine serum (SFB), 2mM L-glutamine and 1% antibiotics (10.000 IU/mL penicillin and 10 mg/mL streptomycin). Culture flasks of 75 cm<sup>2</sup> and kept in an incubator for cell incubation including a humid atmosphere with 5% CO<sub>2</sub>, at 37 °C. Upon reaching an approximate confluence of 90%, the cells were cultured for cell enlargement and freezing. Before carrying out the experiments, the cells were counted in a Neubauer chamber, using trypan blue dye (1%) and the viability was greater than 97%.

### 2.1.2. Evaluation of cytotoxicity by the MTT colorimetric method

Cell viability was assessed by the MTT [3-(4,5-dimethylthiazole-2-yl)-2,5-diphenyltetrazolium bromide] colorimetric reduction test. The cells were grown at a density of 2x10<sup>4</sup>, in 96-well plates, for 24h in an oven at 37°C, containing 5% CO<sub>2</sub>. During 24h the cells were treated with different concentrations (10 µg - 150 µg) of the fractions in the acetate and chloroform preparations. After the treatment period, 10µL of MTT reagent (5 mg/mL) was added and maintained for 3h. Subsequently, the supernatant was removed and 100µL of DMSO was added to dissolve formazan crystals. The absorbance quantification was performed in an ELISA reader (ThermoPlate), at a wavelength of 540nm, for the determination of the inhibitory concentration (IC<sub>50%</sub>) and calculation of the line equation (r<sup>2</sup>).

### 2.1.3. Analysis of mitochondrial electrical potential (ΔΨ<sub>m</sub>) by laser confocal microscopy

The rhodamine-123 probe was used to analyze the mitochondrial potential (ΔΨ<sub>m</sub>) and analyzed by confocal microscopy. B16-F10 and FN1 cells were plated at a concentration of 1x10<sup>5</sup>/well, under round coverslips in 24-well plates. After 24h, the cells were treated with the IC<sub>50%</sub> values of the CHCl<sub>3</sub> and acetate fractions for a period of 12h. During this treatment period, the cells were washed three times with RPMI-1640 culture medium at 37 °C, incubated with 5 µg/mL rhodamine, and placed in the oven for 10 min in the dark. Excess rhodamine was removed by washing with

the culture medium. The slides were assembled with the aid of forceps and the coverslips were transferred to glass slides, fixed with ProLong® stored at -20 °C, in the dark, until the time of reading in the laser confocal microscope (Carl Zeiss LSM 700; Leica, Mannheim, Germany).

### 2.1.4. Analysis of cytoskeleton by laser confocal microscopy

For structural analysis of the microfilaments, Alexa Fluor<sup>™</sup> 488 Phalloidin was used, observed by the laser confocal microscopy technique. Tumor cells B16-F10 were plated at a concentration of 1x10<sup>5</sup>/well, under round coverslips in 24-well plates. After 24h, the cells were treated with the IC<sub>50%</sub> concentration of the Chloroform and Acetate fractions for a period of 12h. Subsequently, they were washed twice with PBS for two minutes at room temperature, fixed in a solution containing 37% formaldehyde (3%), sucrose, and PBS for 10 min, again the cells were washed twice in PBS and permeabilized. After permeabilization, the cells were washed 2 more times and blocked for 30 min at 3% BSA in PBS. After washing, the cells were incubated with 5µg/mL phalloidin for 30 min. Excess phalloidin was removed by washing with PBS solution. The slides were assembled with tweezers and transferred to glass slides, fixed and stored in the dark, until the time of reading in the laser confocal microscope.

### 2.1.5. Analysis of cell cycle phases by flow cytometry

The melanoma tumor cells (B16-F10) were plated in 6-well plates, at 1x10<sup>5</sup> concentrations, and the following day, they were treated with the concentration obtained from the IC<sub>50%</sub> values for 12h. After this period, the tumor cells were counted and the concentration adjusted to 1x10<sup>6</sup> cell/mL. Then, the tumor cells were centrifuged for 10 min at 1200 rpm and the pellet was resuspended in 1 mL of "Cold GM" (6.1 mM glucose, 137mM NaCl; 4.4mM KCl; 14 NaMHP0<sub>4</sub> 1.5Mm; KH<sub>2</sub>PO<sub>4</sub> 0.9mM; EDTA 0.5mM). Then, absolute ethanol was slowly added, the fixed cells were slowly stirred for 30 min and centrifuged with PBS containing 5mM EDTA (Sigma Aldrich, USA) and resuspended in a solution containing PBS (5mM EDTA ) 18 µg/mL of propidium iodide (PI) (Sigma Aldrich, USA) and 0.3 mg/mL of RNase -A. The cells were kept at room temperature for 1h in the dark. The reading was performed by a cytometer (FASC Calibur BD, USA), in the diffraction channel FL2-H.

### 2.1.6. Statistical analysis

The data values were expressed as mean ± deviation (SD). The Kruskal-Wallis test (one-way non-parametric ANOVA) and Dun's multiple comparisons were used to identify the statistical differences between the measurements of the groups studied. The graphics were obtained using the program Prism Version 5.0.

## 3. Result and Discussion

The cytotoxic potential of the Acetate and Chloroform fractions showed a significant reduction in cell density in tumor B16-F10 cells from the concentrations 2.3µg/mL<sup>-1</sup> and 13.7 µg/mL<sup>-1</sup> (Figure 1A and 1B), promoting cytoplasmic retraction and alteration in cell morphology. In addition, the normal fibroblast FN1 cells treated with the fractions, also showed morphological changes and cytoplasmic retraction from the first concentrations, obtaining IC<sub>50%</sub> of 13 µg/mL<sup>-1</sup> for Acetate and 12.2 µg/mL<sup>-1</sup> for Chloroform (Figure 2A and 2B), at the highest concentrations there was cell unviability for both cells, B16-F10 and FN1 (Figures 3 and 4).

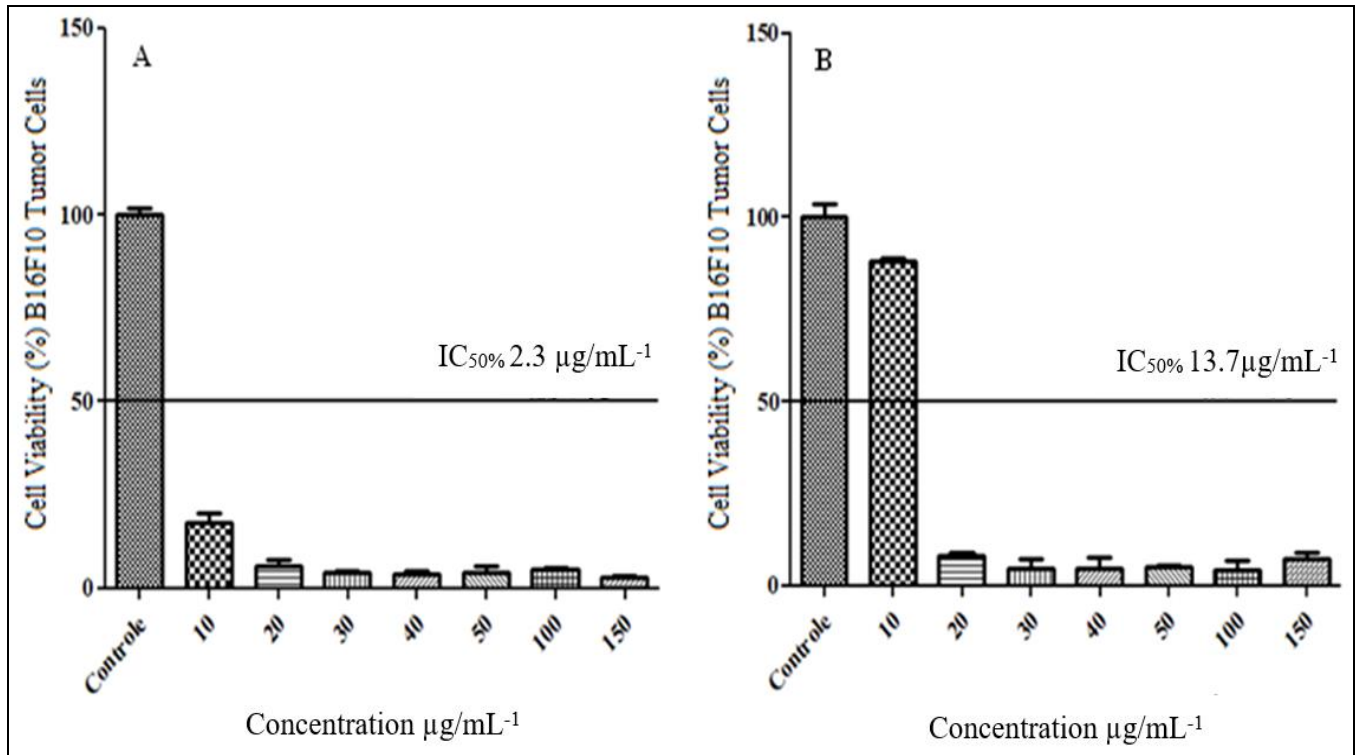


**Fig 1:** Determination of cytotoxicity by the MTT colorimetric method. The graph shows the correlation of the cytotoxic effect expressed as mean  $\pm$  SD of the viability of the B16-F10 melanoma tumor cell after 24h of treatment. (A) Acetate fraction (B) Chloroform fraction. Graphs obtained by the Graph Pad Prism 5 software.

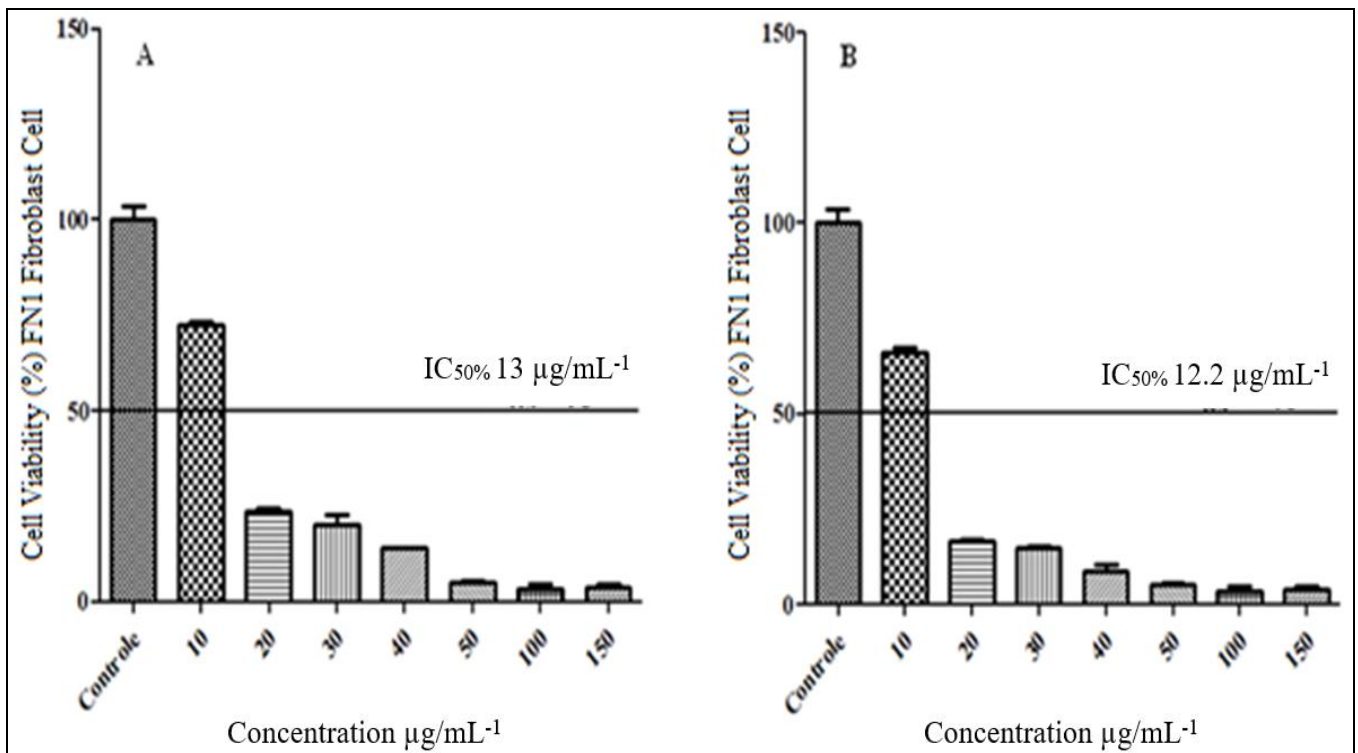


**Fig 2:** Determination of cytotoxicity by the MTT colorimetric method. The graph shows the correlation of the cytotoxic effect expressed as mean  $\pm$  SD of the viability of the normal fibroblast (FN1) cell after 24h of treatment. (A) Acetate fraction (B) Chloroform fraction. Graphs obtained by the GraphPad Prism 5 Software.

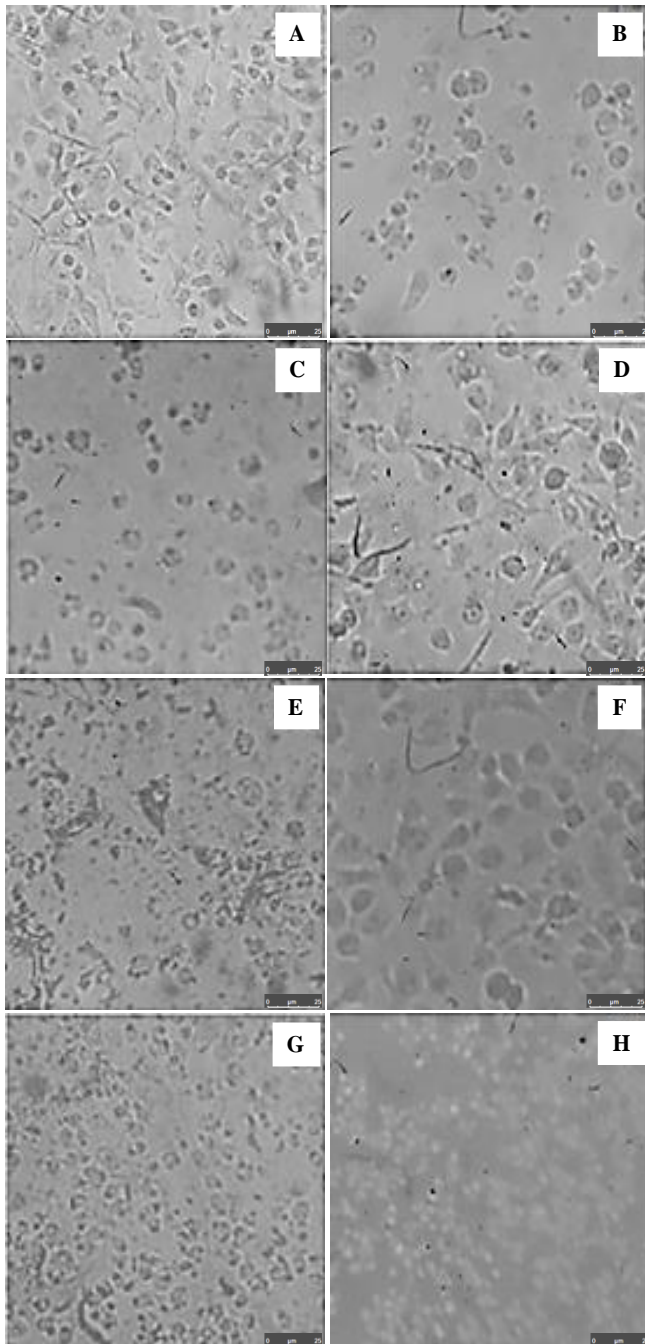


**Fig 3.1:** Photomicrograph of morphological analysis by an inverted microscope. B16-F10 murine melanoma tumor cells after 24h of treatment with Acetate fraction. (A) Control group; (B) 10 μg; (C) 20 μg; (D) 30 μg; (E) 40 μg; (F) 50 μg; (G) 100 μg; (H) 150 μg.

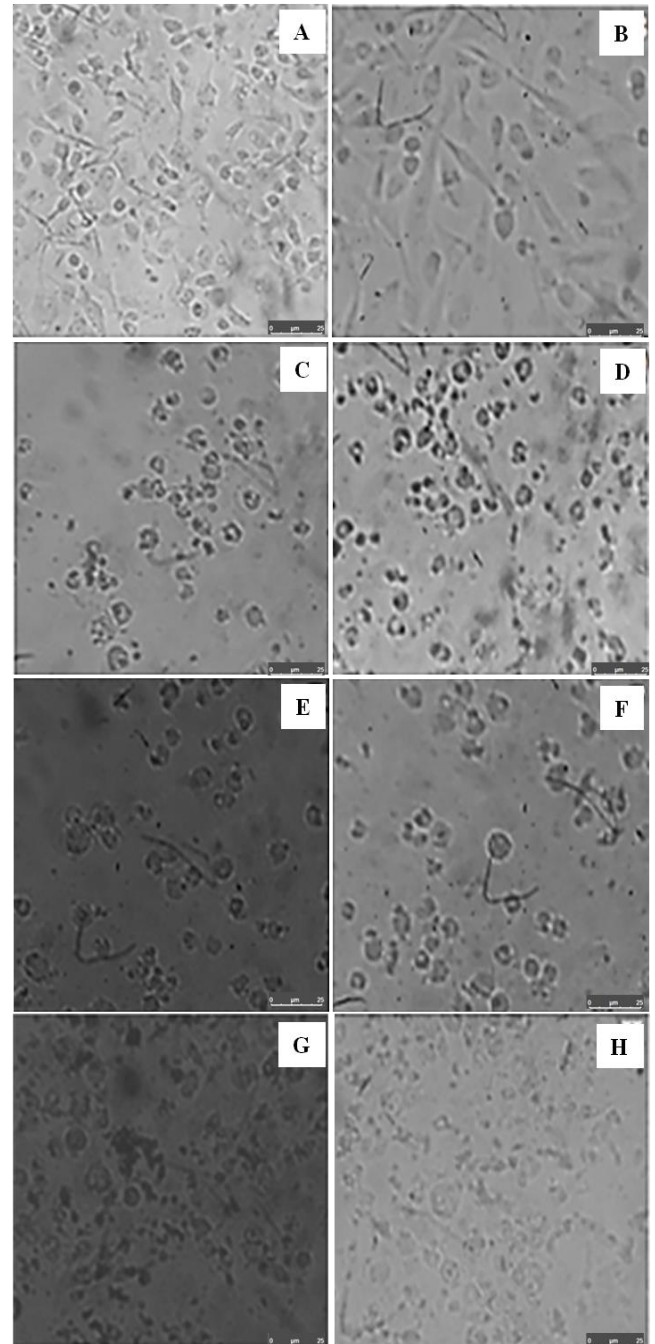


**Fig 3.2:** Photomicrograph of morphological analysis by an inverted microscope. B16-F10 murine melanoma tumor cells after 24h of treatment with Chloroform fraction. (A) Control group; (B) 10μg; (C) 20μg; (D) 30μg; (E) 40μg; (F) 50μg; (G) 100μg; (H) 150μg.

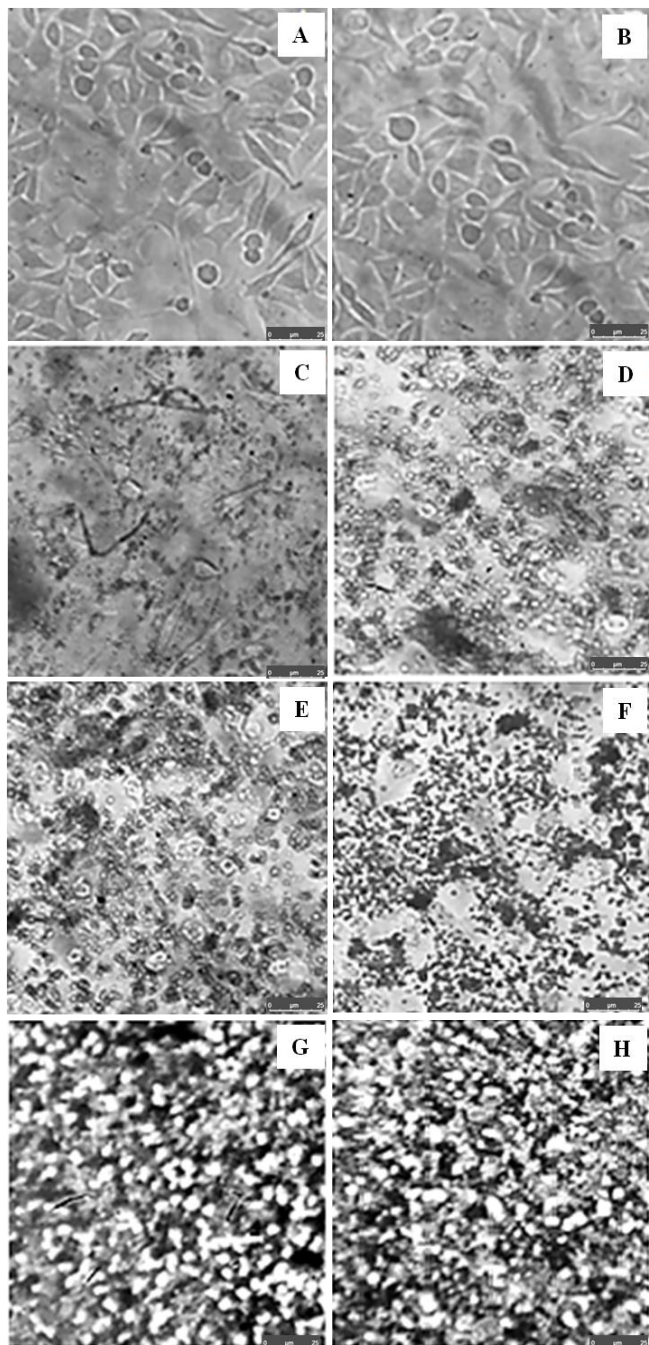


**Fig 4.1:** Photomicrograph of morphological analysis by inverted microscope. FN1 normal fibroblast cells after 24h of treatment with Acetate fraction. (A)Control group; (B)10 µg; (C)20 µg; (D)30 µg; (E) 40 µg; (F)50 µg; (G)100 µg; (H)150 µg.

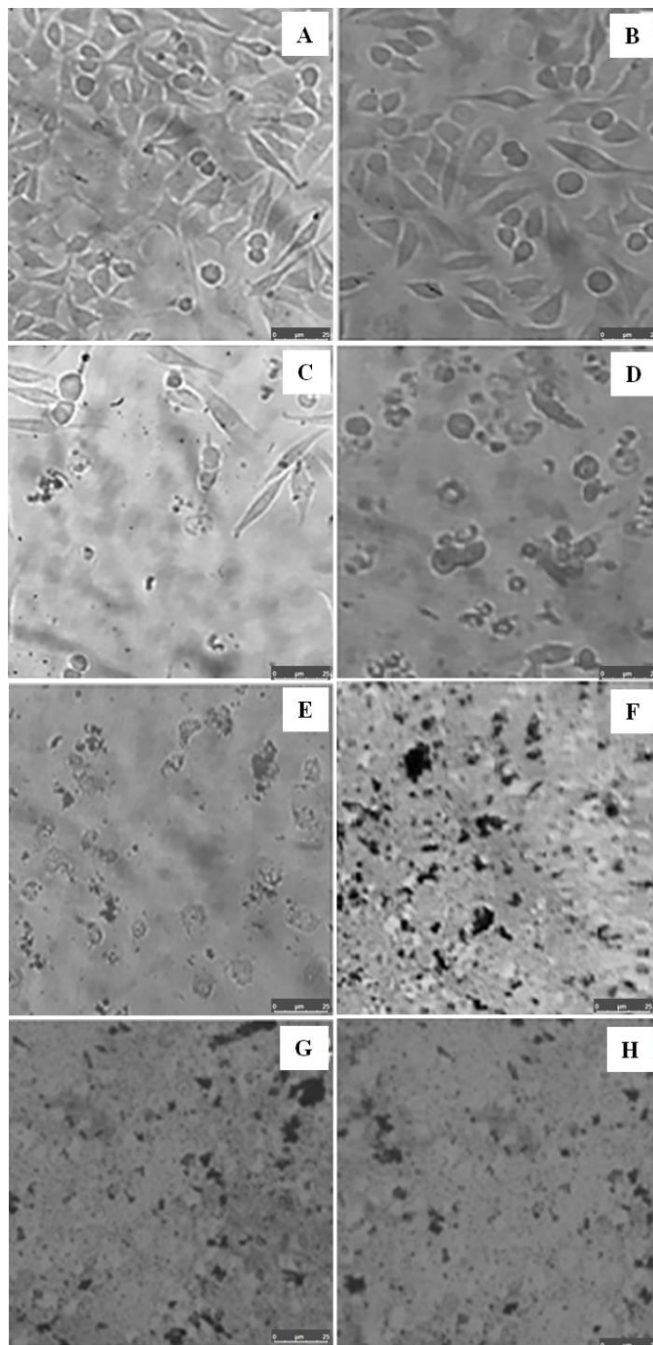


**Fig 4.2:** Photomicrograph of morphological analysis by inverted microscope. FN1 normal fibroblast cells after 24h of treatment with Chloroform fraction. (A)Control group; (B)10 µg; (C)20 µg; (D)30 µg; (E)40 µg; (F)50 µg; (G)100 µg; (H)150 µg.

Similarly to the results obtained, Cabral (2018), showed the cytotoxic effect of the Methanol (MeOH) subfraction from the Hexane (Hex) fraction, extracted from the plant's latex in Hepalcl7 hepatocarcinoma cells where the subfraction presented a potential for in vitro treatment of tumor cells, without presenting cytotoxicity for normal fibroblast FN1 cells.

The results obtained through the rhodamine-123 assay demonstrated greater cytotoxicity of the acetate and chloroform fractions for the B16-F10 tumor cells treated at the concentration of the  $IC_{50\%}$  values (Figure 5B and 5C), when compared to the control group and the treatment for normal FN1 cells (Figure 6), the B16-F10 tumor cells had a significant reduction in  $\Delta\Psi_m$ , mainly in the treatment with the Acetate fraction.

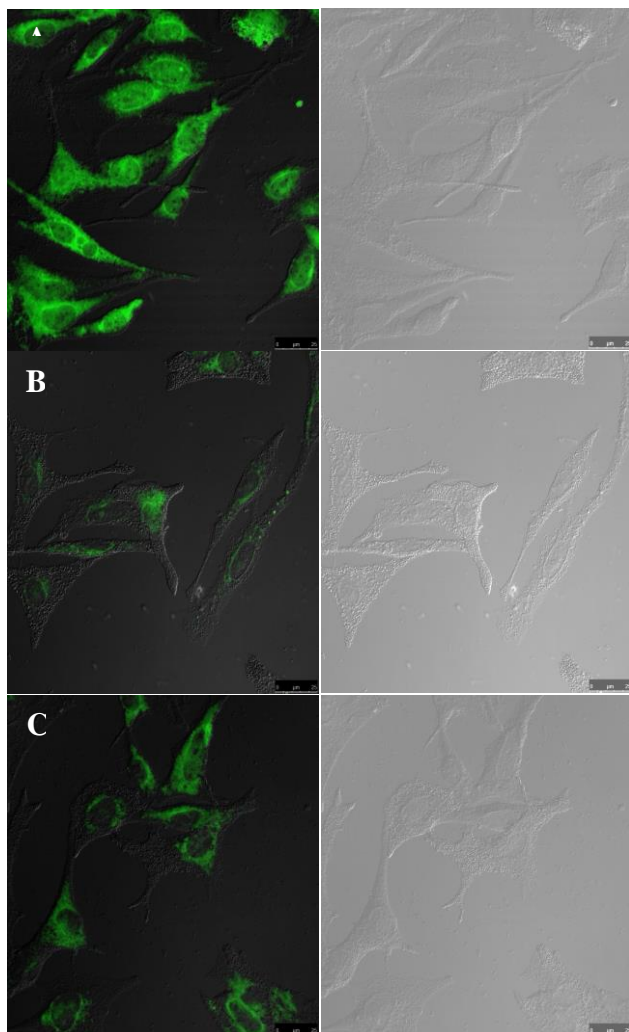


**Fig 5:** Photomicrograph of morphological analysis and mitochondrial electrical potential by confocal microscopy. B16F10 melanoma tumor cells treated with the acetate and chloroform fractions within 24 hours. (A) Control group; (B) Acetate 2.3  $\mu\text{g}$ ; (C) Chloroform 13.7  $\mu\text{g}$ . Photomicrographs without fluorescence to evidence cell morphology and the changes that have occurred.

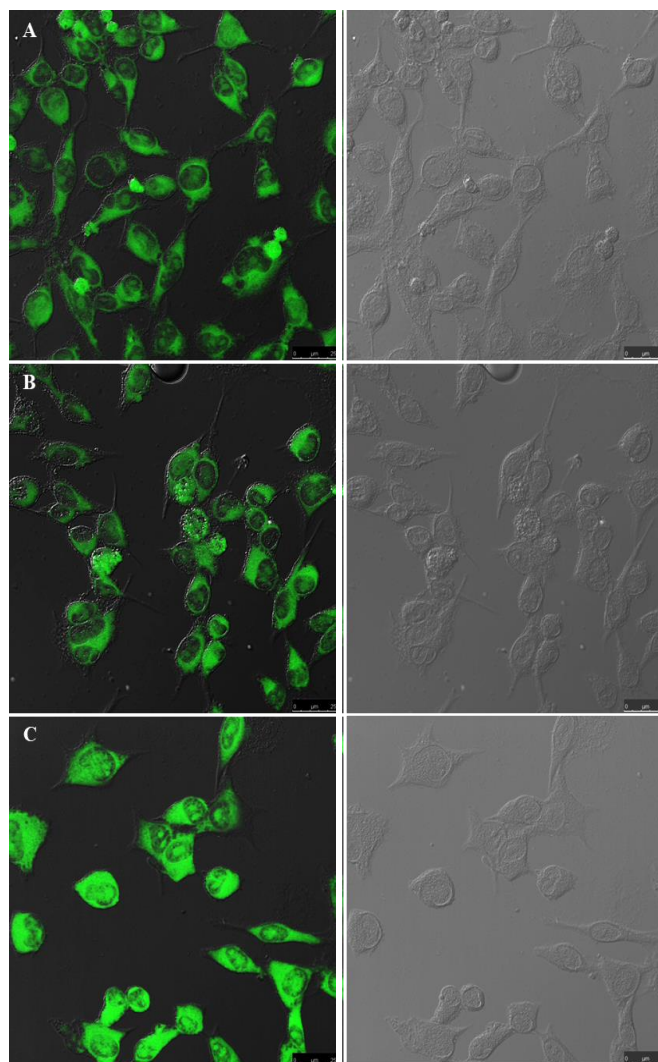


**Fig 6:** Photomicrograph of morphological analysis and mitochondrial electrical potential by confocal microscopy. Normal human fibroblast cells FN1 treated with the acetate and chloroform fractions within 24 hours. (a) control (b) acetate 2.3  $\mu\text{g}$  (c) chloroform 13.7  $\mu\text{g}$ . Photomicrographs without fluorescence to evidence cell morphology and the changes that have occurred.

Previous studies have reported the ability of latex from plants of the Euphorbiaceae family to modulate  $\Delta\Psi_m$ . *Euphorbia antiquorum* latex was able to promote the loss of  $\Delta\Psi_m$  in Hela cells, increase ROS levels and also induce an increase in proteins such as p38 and caspases 8,9 and 3 [17]. that investigated the cytotoxic interference of *E. umbellata* also demonstrated that its extracts were able to decrease the viability of Ehrlich's ascitic tumor cells, with an increase dependent on the time of ROS generation and intracellular  $\text{Ca}^{2+}$  levels [18]. Increased ROS generation has been associated with changes in the integrity of the mitochondrial membrane and  $\Delta\Psi_m$ , the intracellular super generation of ROS is an initial sign of apoptotic processes and a critical determinant of toxicity associated with chemotherapy [19-20].

Chemotherapeutics such as adriamycin and bleomycin, induce apoptosis in tumor cells, increasing the generation of ROS in parallel with the  $\Delta\psi_m$  alteration, in addition, under conditions of oxidative stress, the decrease in mitochondrial function could contribute to apoptosis through the opening of the pore transition of mitochondrial permeability, resulting in mitochondrial release of  $Ca^{2+}$  [21].

Also, it was possible to observe that the actin filaments (Figure 7) underwent significant changes, also showing the formation of stress fibers in the B16-F10 tumor cells treated

with Chloroform (Figure 7C), indicating a cellular dysfunction. Actin is a protein component of the cytoskeleton of eukaryotes and plays important roles in cell dynamics, such as maintaining morphology, mitosis, regulating signaling for survival, and increasing cellular sensitivity to the induction of apoptosis when this protein is aggregated due to its depolymerization [22]. A correlation is likely between the cytotoxic action of the Acetate and Chloroform fractions and their action on the actin filaments, as well as modulation of apoptosis in B16-F10 tumor cells.

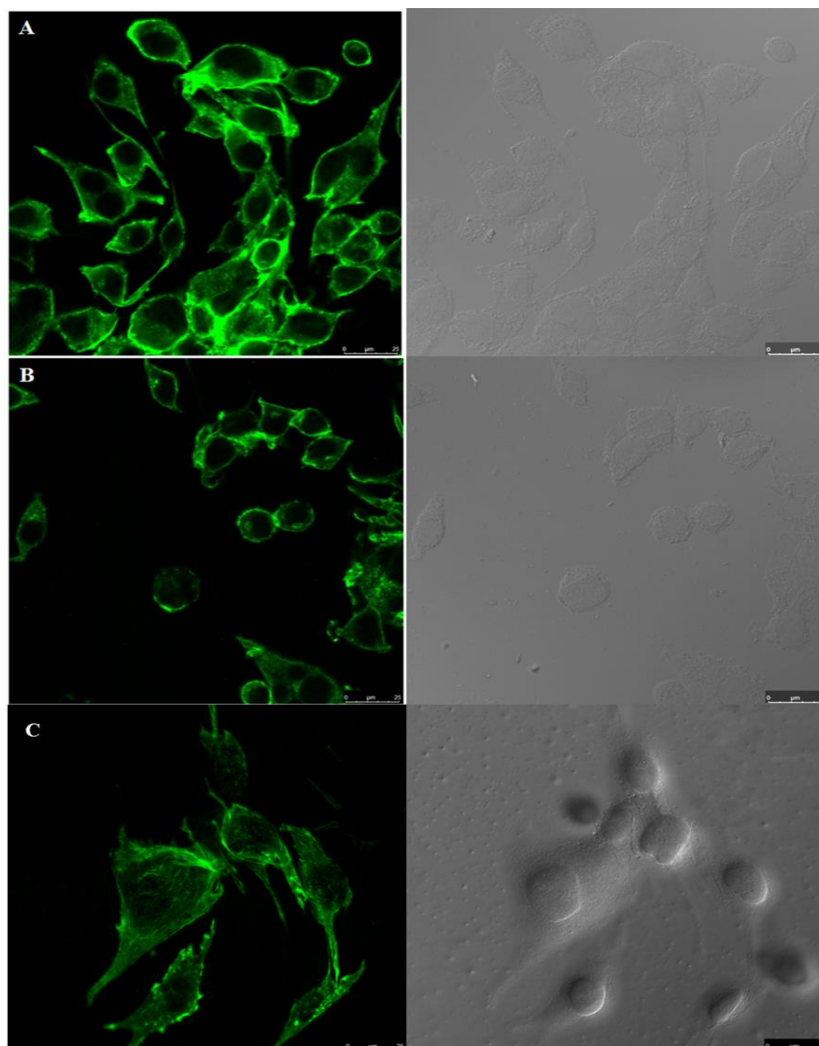


**Fig 7:** Photomicrograph of the analysis of the phalloidin-labeled cytoskeleton by confocal microscopy. B16-F10 melanoma tumor cells treated within 24 hours. (A)Control group; (B) Acetate 2.3 $\mu$ g;(C) Chloroform 13.7 $\mu$ g.

The results obtained showed that the Acetate fraction (Figure 8B) promotes an increase in the cell population with fragmented DNA when compared to the control group (Figure 8A) and the Chloroform fraction (Figure 8B). Yang *et al.* (2016), observed a similar result with the crude extract of *Euphorbia formosana* in prostate cancer cells (DU145) that showed time-dependent DNA fragmentation and damage [23]. Another study carried out with *E. umbellata* on hepatocarcinoma cells (Hepal1c7) and triple negative breast cancer (MDA-MB 231) also showed that the Acetate fraction and the Chloroform fraction significantly increased the cell population with fragmented DNA, when compared to the control for all tumor cells under test [15].

In addition, we observed a decrease in the population of B16-F10 tumor cells that were treated, stopped in the G2/M phase of the cell cycle (Figure 8D), with the Acetate fraction showing  $13.81 \pm 2.3\%$  and the Chloroform fraction showing only  $4.82 \pm 3.7\%$ , compared to the control group  $25.90 \pm 2.9\%$ , a consequence of a significant halt of the cell population in the S phase of the cell cycle in the treatments of the Acetate fraction ( $42.81 \pm 1.4\%$ ) and Chloroform fraction ( $57.43 \pm 2.2\%$ ) probably due to checkpoints between the S and G2/M. This control point is put into operation as a safety mechanism to ensure that changes in the molecular structure of DNA that would cause harmful changes, do not proceed before being repaired, contributing to the maintenance of genomic stability and transmission of mutations to daughter cells [15].

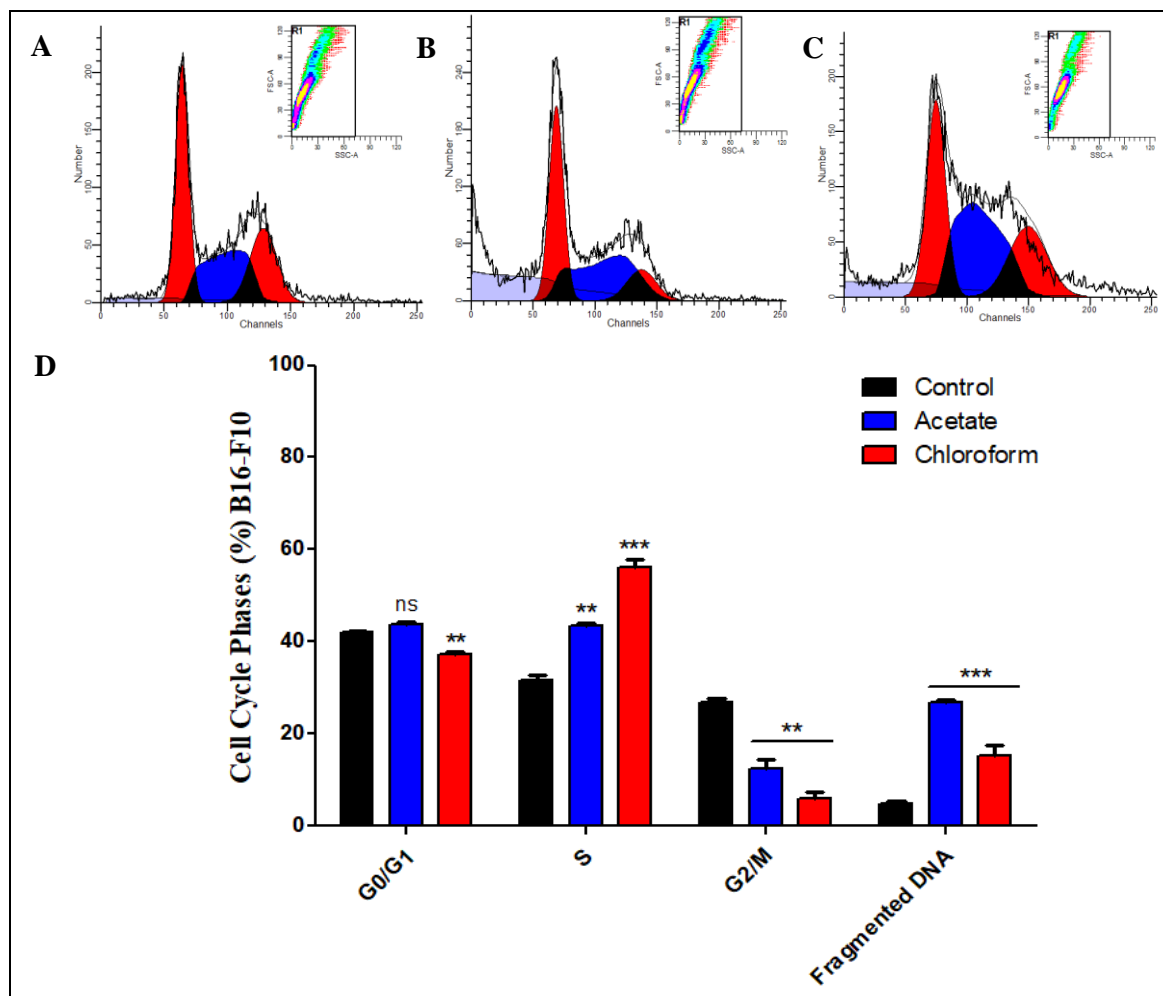


**Fig 8:** Determination of population tumor cells in the cell cycle phases. B16-F10 tumor cells treated with IC<sub>50</sub>% values 24h (A) Control group; (B) Acetate 2.3µg; (C) Chloroform 13.7µg ; (D) Comparative graph of the phases of the cell cycle according to the treatments: Control group, Acetate fraction and Chloroform fraction. Statistical significance level n/s: not significant \*  $p < 0.05$ , \*\*  $p < 0.01$  and \*\*\*  $p < 0.001$ .

#### 4. Conclusion

Our results demonstrate that Acetate e Chloroform fractions present cytotoxicity to the B16-F10 melanoma tumor cell, inhibiting proliferation and causing cell death increasing the number of cells in the G2/M phases of the cell cycle, promoting depolarization and reorganization of the cytoskeleton, as well as potential modulation mitochondrial electrical. The normal fibroblast FN1 cell was more sensitive to treatment with the Chloroform fraction, with no selectivity. In this context, our results suggest that acetate and chloroform can inhibit the proliferation of B16-F10 melanoma tumor cells, promoting apoptosis and control to melanoma tumor cell proliferation. The acetate fraction is promising for melanoma probably by modulating apoptotic pathways and disrupt the cytoskeleton organization.

#### 5. Acknowledgments

Support: CAPES (Coordination for the Improvement of Higher Education Personnel) and CNPQ (National Council for Scientific and Technological Development), number the process CNPQ: 305056/2019-0.

#### 6. Conflict of interest Statement

The authors declare that there are no conflicts of interest.

#### 7. Funding

Coordination of Improvement of Higher Level Personnel and Foundation for Research Support of the State of São Paulo

CNPq processnumber 306124/2015-7.Maria DA.

Higher Education Personnel Improvement Coordination - CAPES

#### 8. References

- Maio M. melanoma as a model tumour for immunoncology. *Annals of oncology* 2012;23(8):10-14.
- Bonalumi A, Campos E, Leal F. *Oncologia Cutanea*. Elsevier Brasil 2017.
- INCA. Estimativa 2018-2019. Ministério da saúde 2017.
- Kom EL, Liu PY, Lee SJ. Meta-analysis of phase II cooperative group trials in metastatic stage IV melanoma to determine progression-free and overall survival benchmarks for future phase II trials. *Journal of Clinical Oncology* 2008;26(4):527-534.
- Bhatia S, Tykodi SS, Thompson JA. Treatment of metastatic melanoma: an overview. *Oncology* 2009;236:488.
- Johnson DB, Sosman JA. Therapeutic advances and treatment options in metastatic melanoma. *Jama oncology* 2015;1(3):380-386.
- Finn L, Markovi SN, Joseph RW. Therapy for metastatic melanoma: the past, present, and future. *BMC medicine* 2012;10(1):23.
- Strickland LR, Pal HC, Elmetts CA, Afaq F. Targeting drivers of melanoma with synthetic small molecules and phytochemicals. *Cancer letters* 2015;359(1):20-35.
- Newman DJ, Cragg GM. Natural products as sources of

- new drugs over the 30 years from 1981 to 2010. Journal of natural products 2012;75(3):311-335.
10. Junior RGO *et al.* Phytochemical analysis and cytotoxic activity of *Cnidioscolus quercifolius* Pohl (Euphorbiaceae) against prostate (PC3 and PC3-M) and breast (MCF-7) cancer cells. Pharmacognosy Magazine 2019;15(60):24.
  11. Santana KCB. Isolamento de gene de defensina em *Euphorbia hyssopifolia* L., caracterização in silico, propriedades químicas e funções putativa da proteína codificada. Universidade Federal de Pernambuco masters dissertation 2012.
  12. Luz LEC *et al.* Cytotoxicity of Latex and Pharmacobotanical Study of Leaves and Stem of *Euphorbia umbellata* (Janaúba). Brazilian Journal of Pharmacognosy 2015;25(4):344-52.
  13. Oliveira TL *et al.* Antitumoural effect of *Synadenium grantii* hook f. (euphorbiaceae) latex. Journal of ethnopharmacology 2013;150(1):263-269.
  14. Luz LEC, *et al.* Cytotoxic biomonitored study of *Euphorbia umpellata* (Pax) Bruyns. Journal of ethnopharmacology 2016;183:29-37.
  15. Cabral LGS, Alves MG, Silva MGL, Cruz LS, Beltrame FL, Luna ACL *et al.* Antitumor potential of *Euphorbia umbellata* latex fractions and subfractions. International Journal of Herbal Medicine 2019;7(5):45-51.
  16. Andrade EA *et al.* Efeito citotóxico do látex de *Euphorbia umbellata* (Pax) Bruyns (Euphorbiaceae) para modelo de melonoma murino. Universidade Estadual de Ponta Grossa masters dissertation 2020,
  17. Hsieh WT *et al.* Latex of *Euphorbia Antiquorum* Induces Apoptosis in Human Cervical Cancer Cells via c-Jun N-Terminal Kinase Activation and Reactive Oxygen Species Production. Nutrition and cancer 2011;63(8):1339-1347.
  18. Mota MF, Benfica PL, Batista AC, Martins FS, Paula JR, Valadares MC. Investigation of Ehrlich ascites tumor cell death mechanisms induced by *Synadennium umbellatum* Pax. Journal of Ethnopharmacology 2012; 139(2):319-329.
  19. Poot M, Pierce RH, Kavanagh TJ. Flow cytometric and fluorometric methods of quantifying and characterizing apoptotic cell death. Humana Press 2002, In: Apoptosis methods in pharmacology and toxicology; 11-36.
  20. Chandra J, Samali A, Orrenius S. Triggers and modulation of apoptosis by oxidative stress. Free radical biology and medicine 2020;29(3-4):323-333.
  21. Kannan K, Jain SK. Oxidative stress and apoptosis. Pathophysiology 2000;7(3):153-163.
  22. Cunha SFG. Modulação de expressão de  $\gamma$ -actina induzida por citrato de ródio em células de carcinoma mamário humano. Universidade de Brasília completion of course work 2017.
  23. Carvalho FP. Avaliação da expressão gênica de vias pró-apoptóticas em células-tronco tumorais de linhagem de câncer de mama triplo-negativo tratadas com fitoestrógenogênese, doxorubicina e radiação ionizante. Universidade de São Paulo doctoral thesis 2016.